COMPARISON OF TWO DISDROMETERS BASED ON DIFFERENT PRINCIPLES

C. CARACCIOLO[1], S. NATALI[2], F. PRODI[1,3], A. TAGLIAVINI[4]

[1] Department of Physics-University of Ferrara, Via Paradiso, 12. 44100-Ferrara
(Italy). Fax: +39-0532-974210. E-mail address: caracciolo@fe.infn.it
[2] Nubila s.a.s., 40128 - Bologna. Via Zago, 2. Fax: +39- 051 - 4150324. E-mail:
natali@nubila.net
[3] ISAC-CNR, 40128 - Bologna. Via Gobetti, 101. Fax: +39-051- 6399647. E-mail:
f.prodi@isac.cnr.it
[4] ADA (Applicazioni Digitali Analogiche) s.r.l., 40128 - Bologna. Via Murri, 86.
Fax: +39 - 051- 6230565. E-mail: tagliavini@adasrl.it

Corresponding author: Clelia Caracciolo

Abstract

The performances of two sensors that measure drop size distributions (DSDs) using different principles and their estimates of rainfall amounts were compared. A classical Joss-Waldvogel disdrometer (JW) and a new instrument named PLUDIX (an X-band raingauge-disdrometer) were used; rainfall rates were also measured by a tipping-bucket raingauge. The instruments were operated during the winter of 2001/2002 at the Department of Physics-University of Ferrara (Ferrara, Italy). Four stratiform rainfall events, one snow event and a rain-hail event were analyzed. It was demonstrated that the number concentration of small diameter drops is underestimated by JW as the rainfall-rate increases and that the long-time-period averaged DSD followed well a gamma distribution. It was also found that the Pludix DSD is better parametrized by an exponential distribution. Pludix for the light rain tested events generally underestimates the rain with respect to the JW disdrometer. Pludix also detects very well snow and hail, that JW does not see. The overall analysis has shown that Pludix has good capabilities in rainfall rate and DSD estimations; its future is to be used as a Present Weather Sensor and to be used in local networks. Different Pludix calibration approaches are however under analysis, to improve its performances.

Keywords: Rainfall, Raindrop size distribution, comparison, Doppler

1. Introduction

Measurements of rain drop size distributions (DSDs) at the surface are fundamental in cloud physics for understanding the microphysics of precipitation and to study the processes (like coalescence and break-up) that modify the raindrop size distribution in the upper levels. Several studies demonstrated that the DSD shows different properties depending upon precipitation processes (see for example Waldvogel (1974) and more recently Tokay and Short (1996; 1999)). The DSD analysis are also necessary in radar-meteorology, for example to derive empirical relationships between radar measurements and rainfall parameters at the ground.

The object of this paper is to compare the performances of two sensors that measure the DSD using different principles. Classically the DSD is measured by an electromechanical disdrometer (Joss and Waldvogel (1967)). More recent devices are an optical spectropluviometer (Knollenberg (1970), Illingworth and Stevens (1987), Hauser et. al. (1984) and Salles et. al. (1998)) and a 2D video disdrometer (Schönhuber et. al. (1994)) that measures in real time not only the DSD but even the velocity distribution of the particles and the oblateness of drops. In this work a classical JW disdrometer and a more recent instrument (Prodi et. al., (1999; 2000a, 2000b)) named Pludix were used. Pludix is a raingauge-disdrometer based on the analysis of an X-band (9.5 GHz) continuos wave radar signal backscattered by hydrometeors. It provides a more detailed information with respect to a classical tipping-bucket raingauge and to disdrometers, giving information about the precipitation type. It is also crucial in a number of applications (agricolture, soil erosion, etc.). The principle of operation is similar to the one of POSS (Sheppard, (1990)). The Doppler frequency shift of the individual drop is transformed in terminal velocity and size of the drop.

The two instruments were operated during winter 2001/2002 at the Physics Department of the University of Ferrara (Ferrara, Italy) with a temporal resolution of one minute. We also make use of a tipping-bucket raingauge. Four light rainfall events (due to the particular scarcity of precipitation of the winter 2001/2002 in Ferrara and in the surroundings) were analyzed. The performances of the two instruments in both rainfall-rate and DSD measurements were compared (see section 3). A snow and a rain-hail event as seen by Pludix were also analyzed. To compare with more accuracy the two instruments we also tested a new approach to the DSD normalization, the scaling-law theory (Sempere Torres et. al., (1994; 1998)). Considered the different nature of the two instruments and the fact that Pludix is still in a calibration and testing phase, the results are encouraging. Different calibration approaches are still under testing and will be only mentioned in this paper.

2. The instruments

The two instruments were operated at the Department of Physics (University of Ferrara) during all the 2001/2002 winter. The measurements were taken at 1 minute interval, for each instrument.

Pludix (PLUviometro-DIsdrometro in X band) is a bistatic Doppler raingauge-disdrometer for monitoring and characterizing atmospheric precipitation at the ground. Its functions are to:

- Identify precipitation type (rain, snow, hail, drizzle..);
- Provide hydrometeor size distribution (for drops, snowflakes, hailstones);
- Measure instantaneous rainfall rate;
- Give the total rainfall in a given time interval.

The detection and characterization of a precipitation is based on the fact that each precipitation type (rain, snow, hail) has its own Doppler spectrum. So for each precipitation type a different algorithm is selected to determine drop size distribution and rain intensity. As a raingauge, Pludix also provides the instantaneous rainfall-rate and the total amount in a given interval, integrating the disdrometric function. As a disdrometer, it measures the size of the hydrometeors falling in a volume (3 m high and 1 m wide) above it. The diametral interval varies from 0.8 to 7.0 mm.

The instrument is made of a sensor located in a waterproof fiberglass container to be placed outside, connected by a cable to the power supply/signal processing unit. The upper part of the container (dome) is shaped in order to minimize dry deposition and snow cover, and can be heated. The length of the cable connecting the sensor with the power supply/signal processing unit can be extended to several tens of meters. The signal processing unit communicates to the outside through a serial port RS232C, which can be used to connect the instrument to the data transmission system (in the field) or to a PC for archiving and visualization (in the lab).

The sensor is an X band continuous wave, low power (10 mW) Doppler radar (9.5 GHz frequency of operation). The MW beam emitted by an upward oriented antenna is backscattered by hydrometeors in free fall. Near the ground each hydrometeor has reached an aerodynamic equilibrium and falls at a constant terminal velocity only as a function of its size. The backscattered signal at the receiving antenna is comprised of many components that are shifted in frequency from the transmitted signal depending on the hydrometeors' terminal velocities (Doppler effect). The amplitude of these components is a function of the reflectivity of the hydrometeors and their concentrations in the volume seen by the sensor. Since a given drop at terminal velocity is not generating a constant but rather a variable Doppler frequency shift depending on its position in space, a special algorithm has been developed which obtains the hydrometeor size distribution from the signal spectrum and hence the parameters characterizing the precipitation.

To better understand the functioning principle, in the following we considered the rain case. As known, drops fall with a terminal velocity that, near the ground, is approximately constant. This velocity depends from the drop dimensions by the empiric Gunn and Kinzer (1949) relationship:

$$v = 9.65 - 10.3e^{-0.6\,D} \quad (\mathrm{m\ s^{-1}}) \qquad 0.6 \le D \le 5.8$$

in which v is the velocity ($\mathrm{m\ s^{-1}}$) and D is the diameter (mm). The drops cause an echo Doppler which frequency shift f is proportional to the terminal velocity v:

$$f = 2\,v / \lambda$$

λ is the radar wave length (in our case $\lambda = 0.0315$ m).

Even for snow and hail empirical relationships between D and v (Pruppacher e Klett (1978)) were proposed. For the dry snow:

$$v = 0.098\,D^{0.31}$$

and for the hail:

$$v = 5.123\,D^{0.5}$$

with v the velocity in m/s and D the flakes dimensions, in mm.

At the Pludix frequencies (9.5 GHz) the Doppler frequencies of all the hydrometeors (snow, rain, hail, …) are between 0 and 1kHz. For simplicity the frequency interval is divided in three parts: a low part, between 0 e 200Hz (snow band); a central part, between 200 and 600Hz (rain band); an high part, over 600Hz (hail band).

The raindrop size distributions have also been measured by the classical JW disdrometer. It's an electromechanical disdrometer that transforms the vertical momentum of a raindrop falling on the sampling area (50 cm^2) into an electrical signal. A 20-channel pulse height analyzer attaches the pulses of the spectrometer to 20 different drop size classes, covering the diameter range from 0.3 to 5.5 mm. For a detailed description of the instrument see Joss and Waldvogel (1967). A correction was applied to the drop size distribution to account for the dead time associated with the recovery time of the disdrometer transducer.

We also used a classical tipping-bucket raingauge, with a resolution of 0.2 mm.

3. Results and discussion

3.a Overview on the data

We selected for our comparison four rainfall events, one rain-hail event and one snow event from all the winter database. The rainfall-rate events were characterized by a light to moderate precipitation due to the scarcity of precipitation of the 2001/2002 winter in Ferrara. Fig. 1 shows the rainfall-rate R (mm/h) as function of time as seen by the JW disdrometer, for the 27th of November 2001. The rainfall-rate never exceeded 4 mm/h for all the four rainfall-rate events. We selected sub-periods of maximum rainfall-rate intensity for each event: 11/27/01 (10.27-11.27), 11/27/01 (17.39-18.28), 01/24/02 (19.50-21.21), 02/07/02 (03.55-04.38).

The corresponding Pludix spectra for the 11/27/01 can be seen in fig. 2. The graph refers to the instant of maximum rainfall-rate. The Pludix precipitation intensity is indicated by the spectrum amplitude, and by the maximum location. The shape of the spectrum has different characteristics, depending on the different precipitation types. The stratiform and winter precipitation has broad maxima. Broad maxima are also found in convective precipitation. Convective precipitation has relatively flattened spectra, with narrowed and emphasized maxima at higher frequencies, often with irregular shape. In the intense precipitation the spectrum is often interrupted with one abrupt decrease, as a step at high frequencies (the limit is about 600 Hz). This is related with largest attainable raindrops (drop break-up).

For all the considered events all the maxima are broad and are confined between 300-500 Hz (as in fig.2), indicating a stratiform precipitation.

A snow event on December 13 2001 and a rain-hail event on February 21 2002 are shown in fig. 3(a) and (b) respectively. The JW disdrometer can't see these events because of the particular functioning principle. From the observed Pludix spectra, the melting snow presents bell-shaped spectra, with a maximum at ~100 Hz, totally in the lower part of the spectrum. The maximum is sometimes shifted toward higher or lower frequencies (150 and 50 Hz), due to different terminal fall velocities. When the snow is dry and light, the Doppler frequencies can be very low (10-20 Hz). The combined presence of dry and wet snow is indicated by a "bimodality" in the spectrum.

In our case, however, the presence in the atmosphere of frozen hydrometeors with low terminal fall velocities, originates an array of peaks in the lowest part of the spectrum, probably indicating a discontinue DSD, with preferential diameters. A possible explanation of this behavior is that there are probably frozen particles consisting of elementary crystal shapes of given diameter values. The fall velocities and consequently the Doppler frequencies have therefore discrete values, giving the typical "bristly" form at the lowest part of the spectrum (typically under 50 Hz).

The second event (fig. 3-(b)) is a strong rainfall event with light hail. Normally the presence of heavy rain with hail is indicated by the high frequency part of the spectrum, with peaks over 600 Hz. In this case the peak is about 550 Hz and less marked, indicating a light hail mixed to heavy rain.

3.b Rainfall-rate and DSD analysis for the precipitation events

Different rainfall integral and DSD parameters were calculated for all the four rainfall-rate events (see tab. 1). An averaged DSD in each time period was considered.

The N_0 (1/mm/m^3) and Λ (1/mm) values of the exponential DSD (Marshall and Palmer (1948)) were calculated by the JW disdrometer by the N(D) values, and by Pludix by a linear regression method. The m, N_0 (1/mm$^{(1+m)}$/m^3) and Λ (1/mm) values of a gamma distribution were calculated by the method of moments following Tokay and Short (1996). The DSD was parametrized by the gamma DSD of Ulbrich (1983):

$$N(D) = N_0\, D^m \exp(-\Lambda D)$$

Because the x-moment of the DSD is, by definition:

$$M_x = \int_{0,\infty} N(D)\, D^x\, dD = N_0\, \Gamma(m+x+1)/\Lambda^{m+x+1}$$

using the M_3, M_4 and M_6 order moments we derived:

$$m=[11G-8+(G^2+8G)^{1/2}]/2(1-G), \text{ with } G=M_4^3/(M_3^2M_6)$$

$$N_0=\Lambda^{m+4}M_3/\Gamma(m+4)$$

$$\Lambda=(m+4)/D_m, \text{ with } D_m=M_4/M_3$$

The rainfall-rate R (mm/h) was calculated by the observed N(D) as:

$$R = (\pi/6)\int_{0,\infty} N(D)D^3v(D)\, dD$$

while the reflectivity Z (dBZ) was calculated by the sixth order moment as follows:

$$M_6 = \int_{0,\infty} N(D)D^6dD$$

here truncated at $D_{min} = 0.3$ mm., $D_{max} = 5.5$ mm. for JW and at $D_{min} = 0.8$ mm., $D_{max} = 7.0$ mm. for Pludix.

The RA (rain amount, mm.) was calculated by:

$$RA=R\ t/60$$

with t the duration of each event in minutes and R the rainfall-rate expressed in mm/h.

3.b.1 Rainfall-rate comparison

In fig. 4 the rainfall-rate given by the two instruments (with points every minute) is shown for the most representative events (11/27/01 a.m. and 02/07/02). Also the correlation coefficient (denoted as r) was calculated and is shown in fig. 4. In fig. 5 the data are presented as number of minutes spent in rainfall-rate classes (from 0.0 to 7.0 mm/h, with 0.5 mm/h steps) for the two instruments.

From fig. 4 and 5 it can be seen that Pludix tends to underestimate the rainfall-rate with respect to JW (see also table 1), except for the second event (7th February) in which we created a characteristic noise file for the specific collocation of the instrument and subtracted it from the original data. In this case Pludix data are very close to the tipping-bucket raingauge data. In any case the correlation between the two instruments is good. Of course the integrated precipitation over each time period is less in Pludix with respect to the JW and the tipping-bucket raingauge.

From table 1 it can also be seen that Pludix tends to underestimate Z (dBZ) with respect to JW. This is probably due to the fact that the minimum diameter detected by Pludix is 0.8 mm and that the total number of drops per unit volume is, for all the analyzed events, always less that the JW counts (not shown).

3.b.2 Drop size distribution comparison

The exponential DSD parameters N_0 (1/mm/m^3) and Λ (1/mm) for Pludix DSD are always greater than the JW parameters (see tab. 1). This is probably due to the fact that Pludix counts many drops in its first two diametral classes and consequently the DSDs are more narrowed (consequence of the minimum detected diameter, equal to 0.8 mm). This behavior is also confirmed by fig. 6 and 7 below in which we compared the DSD of the two instruments for the 11/27/01 (10.27-11.27). This behavior was also found for all the other three precipitation events (not shown). From fig. 6 it can be seen that the drop size distributions for the two instruments are similar for the same diametral classes (a little overestimation of JW with respect to Pludix); JW sees the small drops, while Pludix sees the biggest drops (until 7.0 mm). Considering the two different operational principles and the different integration intervals of the two instruments, this is a good result.

We also found that (fig. 7 (a) and (b): (a) refers to JW, (b) to Pludix) Pludix DSD is better parametrized by an exponential distribution, while the JW DSD is better parametrized by a gamma distribution (the gamma parameters are shown in tab. 1). JW also strongly underestimates small drops, especially for the most intense event (24th January, not shown). In fig. 7 the long-dashed line is the Marshall and Palmer (1948) corresponding to the measured averaged rainfall intensity, while the dotted line is the parametrized gamma DSD (Ulbrich (1983)).

3.c Normalization approach to the drop size distribution analysis

In our work we also tested a new and very interesting approach to the DSD analysis, the scaling-law theory (Sempere Torres et. al. (1994) and (1998)), which allowed us to compare with more accuracy the two instruments. The scaling-law was in fact applied to all the four precipitation events, as seen by JW and Pludix.

4.c.1 Overview on the scaling-law theory and it's application to our database

In the classical methodology for the DSD analysis proposed by Marshall and Palmer (1948), an average DSD is determined for a large number of records stratified by rain rate intervals, usually grouping several storm events and involving as much records as possible, without taking into account their chronological coherence (Sempere Torres et. al., 2000).

Sempere Torres et. al. (1994; 1998) proposed a general formulation of the DSD in terms of the diameter D and of a reference variable, which can be chosen among any integral variable of the DSD. Using the rainfall-rate R, the general formulation of the DSD can be written in the form: $N(D, R)=R^{\alpha} g(D/R^{\beta})$, where α and β are constants and g is the so-called general distribution function, which is independent of R.

In this formulation, any rain bulk variable written as an integral moment of the DSD is powerfully related to the reference variable independently of the particular shape of g. When R is the reference variable, the moment of order n is written as: $\Omega_n = A_n \int_{0,\infty} D^{n} N(D, R)\, dD$, where A_n is a constant taking into account the units, and the power relationship reads: $\Omega_n = c_n R^{\gamma(n)}$, where c_n and $\gamma(n)$ are coefficients. The exponent $\gamma(n)$ does not depend on g and depends linearly only on the moment order n.

The coefficients of this linear relation are the constants α and β of the general formulation: $\gamma(n)=(n+1)\beta+\alpha$. On the other hand, the coefficient c_n depends on both g and the order n, but as the exponent $\gamma(n)$, it does not depend on the reference variable R: $c_n = A_n \int_{0,\infty} x^{n} g(x)\, dx$. The degree of freedom of the last two expressions is reduced by 2 if the self-consistency requirement is imposed. If the expression $v(D)=3.778D^{0.67}$ is used for the terminal velocity and $\Omega_n = R$, the following constraints must be satisfied:

$$\alpha+4.67\beta=1$$

$$\int_{0,\infty} x^{3.67} g(x)\, dx = 3x10^{-8}$$

The exponents α and β are thus related and there is a constraint for g(x).

As evidenced before, since a rain period can be composed of several phases, each with a different predominant rain mechanism, an average DSD is also probably not the best description. In this general formulation it is possible to fit the most convenient N(D, R) without averaging or splitting the data into classes of R, allowing the data to keep their sequential coherence.

To compute the first moments (n=0,1,2,3,4,5,6) and the corresponding reference variable R, we used the $\Omega_n = A_n \int_{0,\infty} D^n N(D, R)dD$ for each of the four analyzed events. A power function ($\Omega_n = c_n R^{\gamma(n)}$) is fitted for each moment order n. The exponents $\gamma(n)$ of these power functions are related to (n+1) via: $\gamma(n)=(n+1)\beta+\alpha$, which, according to Sempere Torres et. al. (1994; 1998), makes it possible to identify the values of α and β by linear regression.

Once the experimental values of α and β are determined for the considered event, g(x) can be derived by: $g(x)=N(D, R)/R^{\alpha}$, with $x=D/R^{\beta}$. Fig. 8 (b) shows the experimental scaled concentration of drops g(x) versus the scaled diameter x for the 11/27 p.m. event (g(x) is obtained by scaling the 50 1-min recorded spectra), for both

JW and Pludix (crosses=JW; squares=Pludix). From fig. 8 (b) it can be noted the less dispersity of the distribution due to the normalization. Even with the normalization, the JW DSD tends to be of the gamma type, while the Pludix DSD tends to be of an exponential type. It can also be noted the cut of the smallest drops in Pludix, due to its functioning principle. The two distributions are also quite similar for the same diametral classes. This is also true for the other three precipitation events (not shown).

We also tested the validity of the formulation applied to our database, verifying the self-consistency equation (fig. 8 (a)). All the events stay in fact very well on the self-consistent line, both for JW and Pludix. The circle at the point with coordinates $(\alpha,\beta) = (-0.27,0.27)$ corresponds to a situation of purely raindrop size-controlled rainfall (Uijlenhoet (1999)), the cross at the point with coordinates $(\alpha,\beta) = (0,0.21)$ to Marshall and Palmer's (1948) exponential raindrop size distribution, and the circle at the point with coordinates $(\alpha,\beta) = (1,0)$ to purely raindrop concentration-controlled conditions. From fig. 8 (a) we can see that Pludix data, for which α and β are all confined in the right part of the spectrum, must originate from more raindrop concentration-controlled conditions than Marshall and Palmer's (1948) data. All the spatial and temporal variability of the DSD is therefore controlled by raindrop concentration variability (D is in average constant). Uijlenhoet (1999) argues that pure size-control may occur during orographic conditions, pure number-control during equilibrium conditions, and different combinations of size-control and number control during stratiform and convective conditions (with the former predominantly size-controlled and the latter predominantly number-controlled). In our case the Pludix behavior is probably due to the inversion algorithm and to the characteristics of the diametral intervals, different from JW. We are working on overcoming this problem.

4. Conclusions

Two disdrometers based on different principles were compared: a classical JW disdrometer and Pludix (raingauge-disdrometer in X-band, 9.5 GHz) a new instrument that has the capability to monitor precipitation, identify the precipitation type (rain, snow, hail, drizzle..) and provide hydrometeor size distribution and instantaneous rainfall rate measurements. The instruments were collocated at the Physics Department of the University of Ferrara (Ferrara, Italy). Four rainfall-rate events occurred in the 2001/2002 winter were analyzed, comparing the performances of the two instruments in both rainfall-rate and DSD measurements. The events were characterized by light rain, because of the particular scarcity of precipitation of the 2001/2002 winter in Ferrara. The most important rainfall integral parameters (like R and Z) and the DSD parameters were analyzed. The DSD was parametrized by an exponential and a gamma distribution. It was found that Pludix DSD is better parametrized by an exponential distribution, while the JW DSD by a gamma distribution. This depends by the fact that Pludix counts drops larger than 0.8 mm. diameter, while JW 0.3 mm.; the elimination of the smallest drops in Pludix gives a distribution near to an exponential form. For the same diametral classes the two instruments have similar DSD. In other words Pludix, underestimating the smallest drops with respect to JW, gives rainfall-rate values lightly less that JW, at least for light precipitation events, like those analyzed in this paper. It is presumable that in intense rainfall-rate events, the situation will invert, because Pludix determines the DSD until 7 mm. of diameter. In future works we plan to make the comparison of high intensity rainfalls.

These considerations are also verified by the rainfall-rate measurements of the two instruments: the JW rainfall-rate is nearly always greater than Pludix and closest to the tipping-bucket raingauge values. In the 7th of February 2002 we found a better agreement between Pludix and the tipping-bucket raingauge; Pludix was in fact perfected with the elimination of the ground noise. The reflectivity values of the two instruments are quite close; however, because of the light rainfall-rate intensity of the analyzed events, and because Pludix counts drops beginning from 0.8 mm. of diameters, the reflectivity of Pludix is always less that the JW reflectivity. In the 7th of February 2002 case the difference is relatively less marked, confirming the improvement of the Pludix performances. We also analyzed a snow and a rain-hail events, that JW is not capable of measuring, showing the good performances of Pludix in detecting such events. To better compare the performances of the two instruments, we also tested a new normalization approach to the DSD analysis (Sempere Torres et. al. (1994; 1998)). We found that Pludix data must originate from more raindrop concentration-controlled conditions than Marshall and Palmer's (1948) data. All the spatial and temporal variability of the DSD is therefore controlled by raindrop concentration variability (D is in average constant). The Pludix behavior is probably due to the inversion algorithm and to the characteristics of the diametral intervals, different from JW. Future works aim at overcoming this problem.

The overall analysis has in conclusion demonstrated the good capability of Pludix in evidencing the rainfall intensity and the size distribution with high accuracy, if compared with a classical disdrometer and a raingauge. At the moment it’s being testing a new signal inversion algorithm that will allow to count drops in the whole diametral interval 0.3-7.0 mm. We expect that this will lead to more accurate results.

The analysis has also demonstrated that Pludix can easily discriminate between any type of hydrometeors (like hail, graupel, snow, drizzle, …); while other classical disdrometer or raingauge does not do.

We expect that Pludix will be particularly suitable for simultaneous control of large remote areas, investigating time and space variability of the events. It could therefore be considered as a Present Weather Sensor (PWS). Further investigations and calibration procedures will lead to improvements in the instrument performances, especially at larger sizes of drops.

References

Gunn R., Kinzer G. D., 1949. The terminal velocity of fall for water droplets in stagnant air. J. Meteor. 6, 243-248.

Hauser D., Amayenc P., Nutten B., Waldtenfel P., 1984. A new optical instrument for simultaneous measurements of raindrop diameter and fall speed disdtributions. J. Atm. Oc. Tech. 1, 256-269.

Illingworth A.J., Stevens C.J., 1987. An optical disdrometer for the measurement of raindrop size spectra in windy conditions. J. Atm. Oc. Tech. 4, 411-421.

Joss J., Waldvogel A., 1967. Ein Spektrograph für Niederschlogstropfen mit automatischer auswertung. Pure Appl. Geophys. 68, 240-246.

Knollenberg R.G., 1970. The optical array: an alternative to scattering or extinction for airborne particle size determination. J. Appl. Met. 9, 86-103.

Marshall J.S., Palmer W. M., 1948. The distribution of raindrops with size. J. Meteor. 5, 165-166.

Prodi, F., Pasqualucci F., Tagliavini A., 1999. Apparecchiatura pluviometrica disdrometrica ad elevata sensibilità e velocitá di risposta. Patent n. MI99A001906.

Prodi, F., Tagliavini A., Pasqualucci F., 2000a. Pludix: an X–band sensor for measuring hydrometeors size distributions and fall rate, Proc. 13th ICCP, 338-339.

Prodi, F., Tagliavini A., Pasqualucci F., 2000b. Time variability in rainfall events observed by Pludix. Phys. Chem. Earth (B), 25, n. 10-12, 959-963.

Pruppacher H.R., Klett J.D., 1978. Microphysics of clouds and precipitation. Reidel, Dordrecht, 714 pp.

Salles C., Creutin J.D., Sempere Torres D., 1998. The optical spectropluviometer revisited. J. Atm. Oc. Tech. 15, 1215-1222.

Sheppard B.E., 1990. The measurement of raindrop size distributions using a small Doppler radar. J. Atm. Oc. Tech., 7, 255-268.

Schönhuber M., Urban H.E., Poiares Baptista J.P.V., Randeu W.L., Riedler W., 1994. Measurements of precipitation characteristics by a new disdrometer. Proc. of Atm. Phys. and Dyn. in the analysis and prognosis of precipitation fields. Rome (I). 15-18 Nov. 1994.

Sempere Torres D., Porrá J., Creutin J.D., 1994. A general formulation for rain drop size distribution. J. Appl. Met. 33, 1494-1502.

Sempere Torres D., Porrá J., Creutin J.D., 1998. Experimental evidence of a general description for raindrop size distribution properties. J. Geoph. Res. 103, D2, 1785-1797

Sempere Torres D., Sánchez-Diema R., Zawadzki I., Creutin J.D., 2000. Identification of stratiform and convective areas using radar data with application to the improvement of DSD analysis and Z-R relations. Phys. Chem. Earth (B). 25, No. 10-11, 985-990.

Tokay A., Short D., 1996. Evidence from tropical raindrop spectra of the origin of rain from stratiform versus convective. J. Appl. Meteor. 35, 355-371.

Tokay A., Short D., 1999. Tropical rainfall associated with convective and stratiform clouds: intercomparison of disdrometer and profiler measurements. J. Appl. Met. 38, 302-320.

Uijlenhoet, 1999. Parameterization of rainfall microstructure for radar meteorology and hydrology. PhD Thesis, Wageningen University, the Netherlands, 279 pp.

Ulbrich C., 1983. Natural Variations in the analytical form of the raindrop size distribution. J. Clim and Appl. Met. 22, 1764-1775.

Waldvogel A., 1974. The N_0 jump of raindrop spectra. J. Atmos. Sci. 31, 1067-1078.

TABLES

Tab.1: Integral and DSD parameters for all the four precipitation events

11/27/01 (10.27-11.27)	**JW**	**Pludix**	**Tipping-bucket**
Time (min)	61	61	61
R (mm/h)	0.83	0.63	0.98
RA (mm)	0.84	0.64	1.0
Z (dBZ)	23.07	21.37	/
N_0 *(mm^{-1}m^{-3})*	5874.43	3.66E+5	/
Λ *(mm^{-1})*	4.41	6.17	/
m (-)	4.35	9.36	/
N_0 *(mm$^{-1-\mu}$m^{-3})*	1.94E+5	1.45E+7	/
Λ *(mm^{-1})*	7.45	11.86	/

11/27/01 (17.39-18.28)	**JW**	**Pludix**	**Tipping-bucket**

Time (min)	50	50	50
R (mm/h)	1.55	1.43	1.68
RA (mm)	1.29	1.19	1.4
Z (dBZ)	27.65	25.73	/
N_0 $(mm^{-1}m^{-3})$	4775.08	2.53E+6	/
Λ (mm^{-1})	3.48	5.71	/
m (-)	3.76	6.65	/
N_0 $(mm^{-1-\mu}m^{-3})$	4.51E+4	1.33E+6	/
Λ (mm^{-1})	5.79	8.89	/

01/24/02 (19.50-21.21)	**JW**	**Pludix**	**Tipping-bucket**
Time (min)	92	92	92
R (mm/h)	2.04	1.81	2.08
RA (mm)	3.13	2.77	3.2
Z (dBZ)	28.01	26.91	/
N_0 $(mm^{-1}m^{-3})$	6665.21	3.36E+5	/
Λ (mm^{-1})	3.52	4.56	/
m (-)	4.30	5.35	/

$N_0\ (mm^{-1-\mu}m^{-3})$	1.02E+5	5.41E+5	/
$\Lambda\ (mm^{-1})$	6.28	7.80	/

02/07/02 (03.55-04.38)	**JW**	**Pludix**	**Tipping-bucket**
Time (min)	44	44	44
R (mm/h)	0.94	1.07	1.09
RA (mm)	0.69	0.78	0.8
Z (dBZ)	26.03	25.01	/
$N_0\ (mm^{-1}m^{-3})$	5184.35	4.04E+5	/
$\Lambda\ (mm^{-1})$	4.01	4.58	/
m (-)	2.39	4.11	/
$N_0\ (mm^{-1-\mu}m^{-3})$	8.29E+3	9.28E+4	/
$\Lambda\ (mm^{-1})$	4.67	6.65	/

FIGURE CAPTIONS

Fig. 1: Overall rainfall-rate R (mm/h) as function of time as seen by the JW disdrometer, for the 11/27/01 a.m. event.

Fig. 2: Output of Pludix for the 11/27/01 a.m. rainfall-rate event at the peak time interval: 1.) power spectrum in the running time interval (1 min), 100 Hz/div in abscissa; 2.) power spectrum in the size ranges; 3.) logarithmic presentation of drop concentration vs size. The blue line shows the MP distribution for the given precipitation intensity; 4.) precipitation intensity vs time (1div, 1 min).

Fig. 3: Two events occurred on winter 2001-2002 and recorded by Pludix: A) snow event on December 13 2001; B) strong rainfall/hail event on February 21 2002.

Fig. 4: Rainfall-rate as function of time for JW (circles) and Pludix (triangles) for the 11/27/01 a.m. and 02/07/02 events. Also the correlation coefficient was calculated.

Fig. 5: Counts in rainfall rate classes (from 0.0 to 7.0 mm/h, with 0.5 mm/h steps) for the two instruments for the 11/27/01 a.m. and 02/07/02 events.

Fig. 6: Comparison of the DSDs of the two instruments for the 11/27/01 a.m. event.

Fig. 7: DSDs of the two instruments ((a)=JW, (b)=Pludix) for the 11/27/01 a.m. event. The long-dashed line is the MP corresponding to the measured averaged rainfall intensity, while the dotted line is the parametrized gamma DSD (Ulbrich, 1983)

Read-Error

Fig. 8: The normalization approach following the scaling-law theory of Sempere Torres et. al. (1994): (a) relationship between α and β parameters for all the analyzed events as seen by JW (blue) and Pludix (green); (b) example of the normalized distribution g(x) vs. x for the 11/27/01 p.m. (crosses = JW; squares = Pludix).

FIGURES

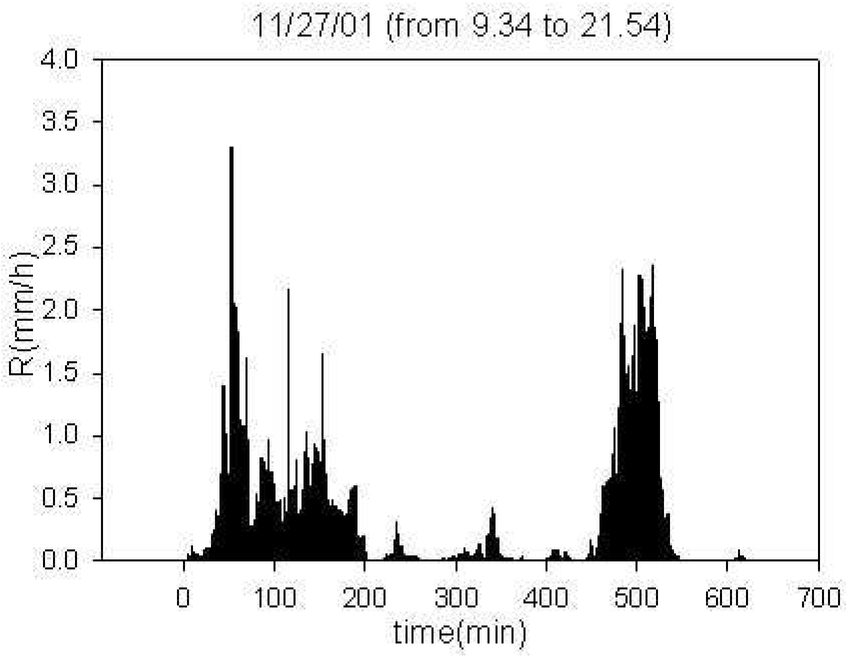
11/27/01 (from 9.34 to 21.54)
R(mm/h)
4.0
3.5
3.0
2.5
2.0
1.5
1.0
0.5
0.0
0
100
200
300
400
500
600
700
time(min)

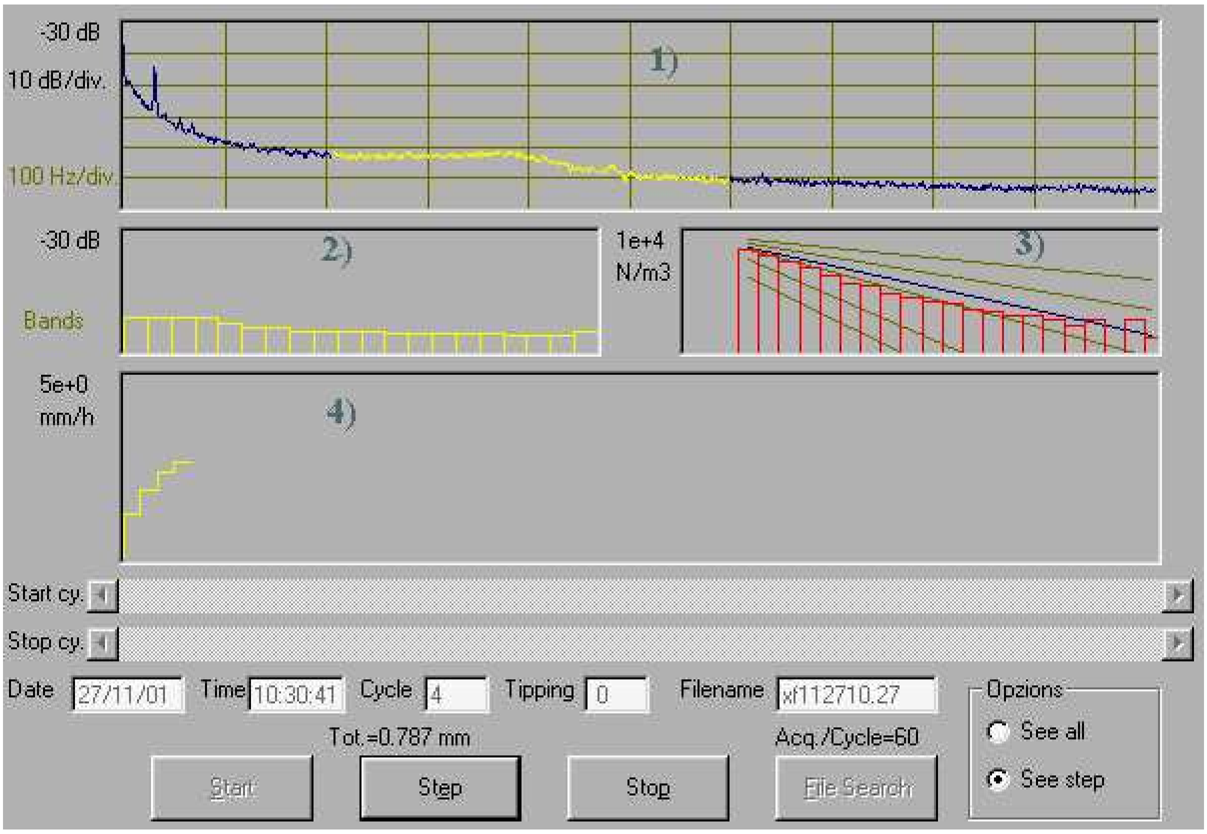

Date 27/11/01 Time 10:30:41 Cycle 4 Tipping 0 Filename xf112710.27

Tot.=0.787 mm

Acq./Cycle=60

Opzions
○ See all
● See step

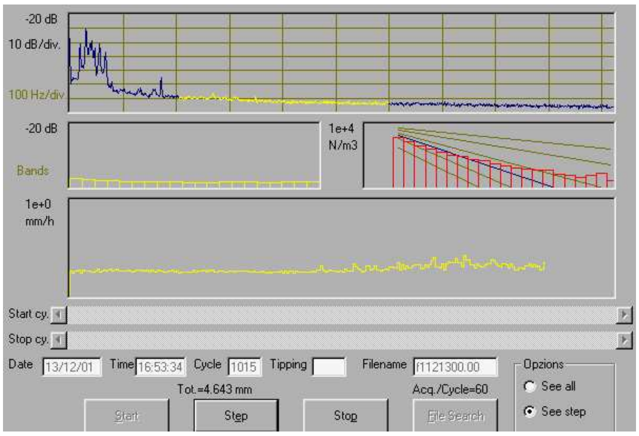

Date 13/12/01 Time 16:53:34 Cycle 1015 Tipping Filename f1121300.00

Tot.=4.643 mm

Acq./Cycle=60

Opzions
○ See all
● See step

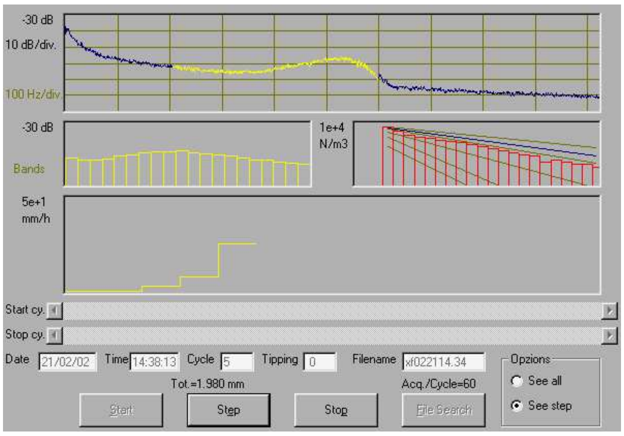

Date 21/02/02 Time 14:38:13 Cycle 5 Tipping 0 Filename xf022114.34

Tot.=1.980 mm

Acq./Cycle=60

Opzions
○ See all
● See step

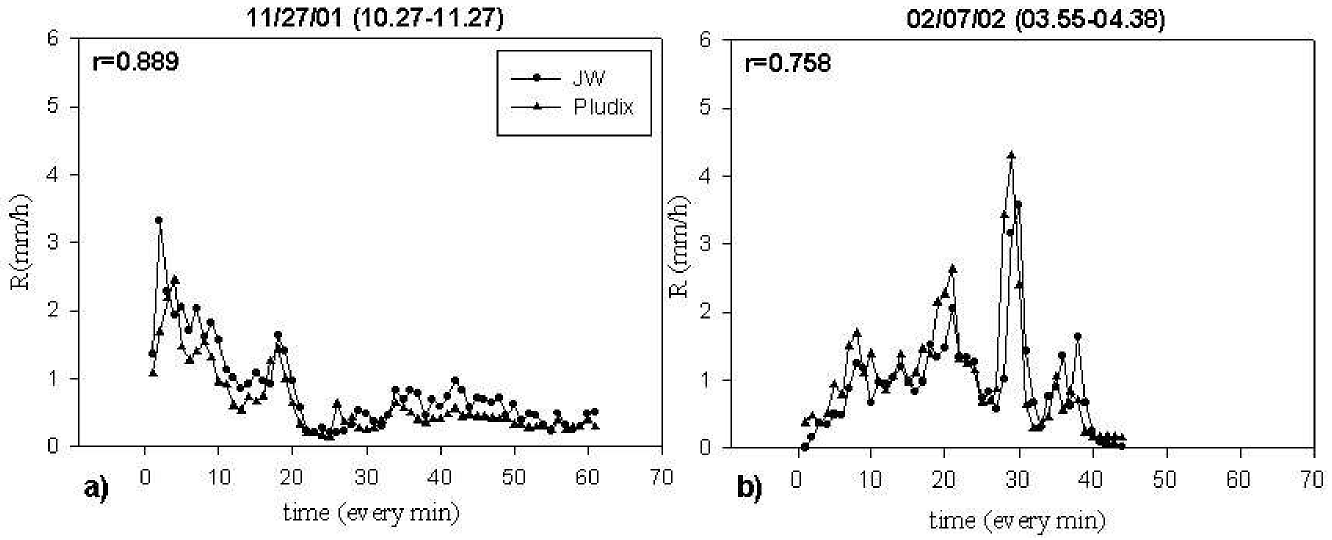
11/27/01 (10.27-11.27)
r=0.889
JW
Pludix
R(mm/h)
0
1
2
3
4
5
6
0
10
20
30
40
50
60
70
time (every min)
a)
02/07/02 (03.55-04.38)
r=0.758
R (mm/h)
0
1
2
3
4
5
6
0
10
20
30
40
50
60
70
time (every min)
b)

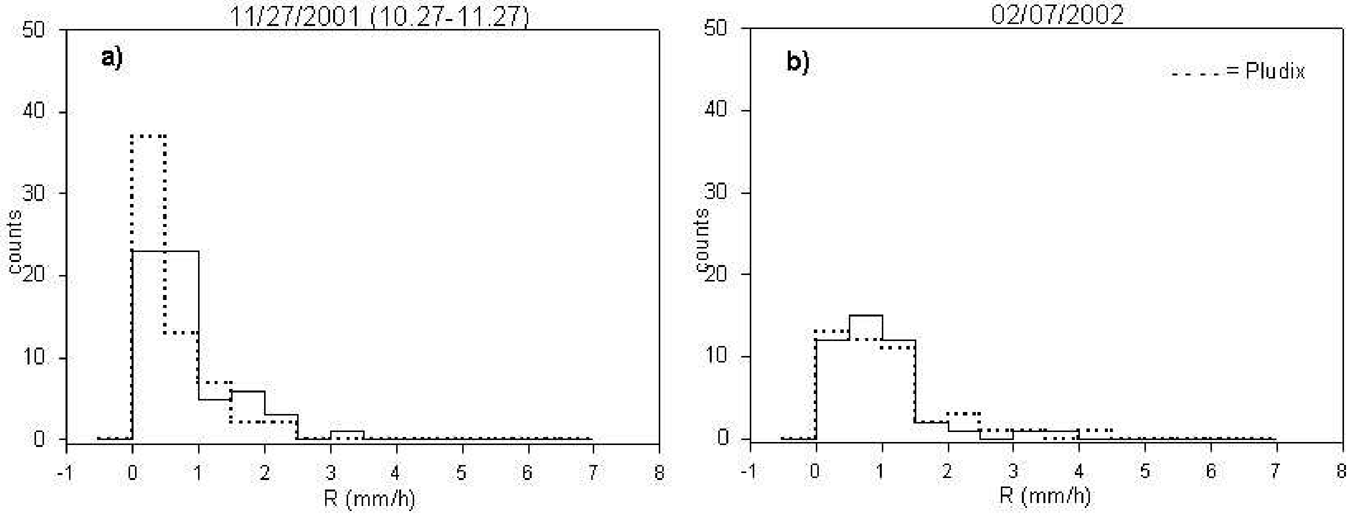
11/27/2001 (10.27-11.27)
a)
counts
0
10
20
30
40
50
-1
0
1
2
3
4
5
6
7
8
R (mm/h)
02/07/2002
b)
- - - - = Pludix
counts
0
10
20
30
40
50
-1
0
1
2
3
4
5
6
7
8
R (mm/h)

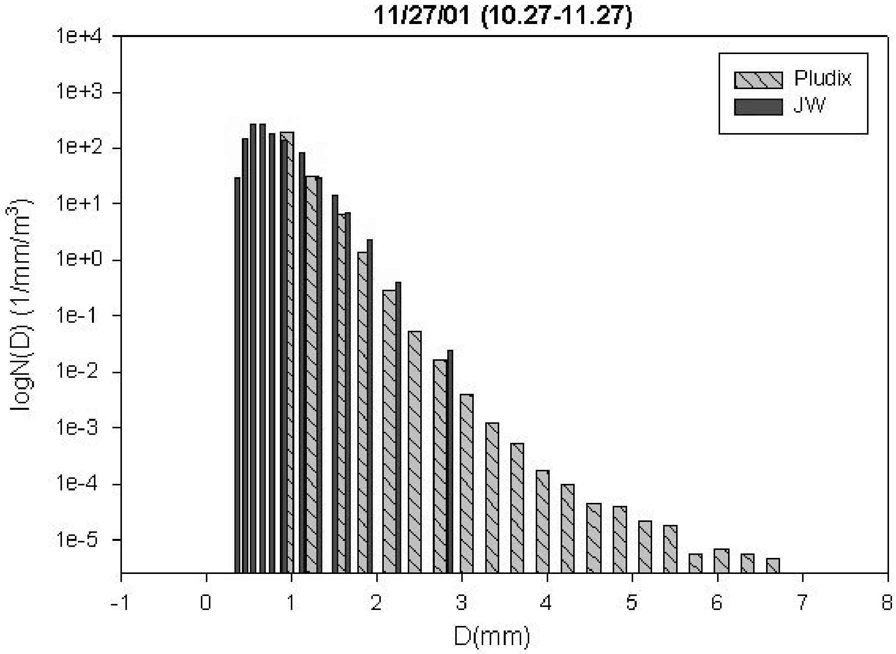
11/27/01 (10.27-11.27)
Pludix
JW
logN(D) (1/mm/m^3)
1e+4
1e+3
1e+2
1e+1
1e+0
1e-1
1e-2
1e-3
1e-4
1e-5
-1
0
1
2
3
4
5
6
7
8
D(mm)

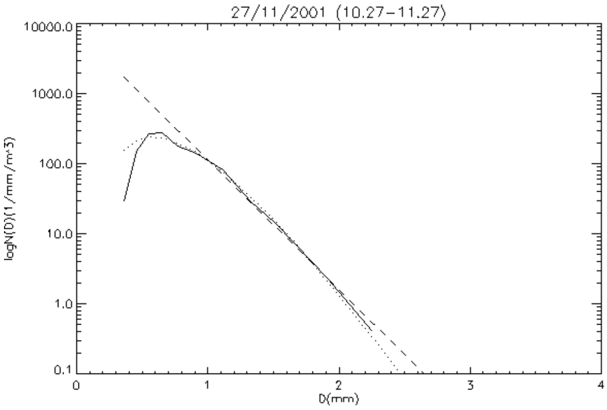
27/11/2001 (10.27-11.27)
logN(D)(1/mm/m^3)
10000.0
1000.0
100.0
10.0
1.0
0.1
0
1
2
3
4
D(mm)

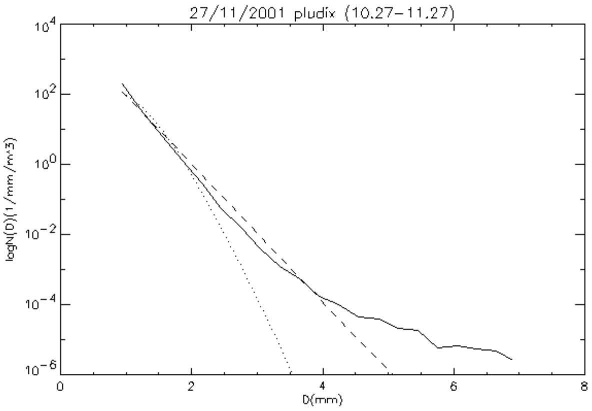
27/11/2001 pludix (10.27-11.27)
logN(D)(1/mm/m^3)
10^4
10^2
10^0
10^{-2}
10^{-4}
10^{-6}
0
2
4
6
8
D(mm)

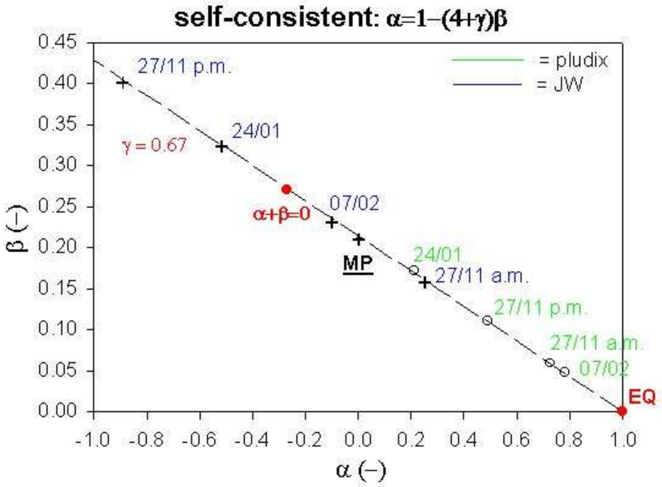
self-consistent: α=1−(4+γ)β
= pludix
= JW
27/11 p.m.
24/01
γ = 0.67
α+β=0
07/02
MP
24/01
27/11 a.m.
27/11 p.m.
27/11 a.m.
07/02
EQ
β (−)
α (−)
0.45
0.40
0.35
0.30
0.25
0.20
0.15
0.10
0.05
0.00
-1.0
-0.8
-0.6
-0.4
-0.2
0.0
0.2
0.4
0.6
0.8
1.0

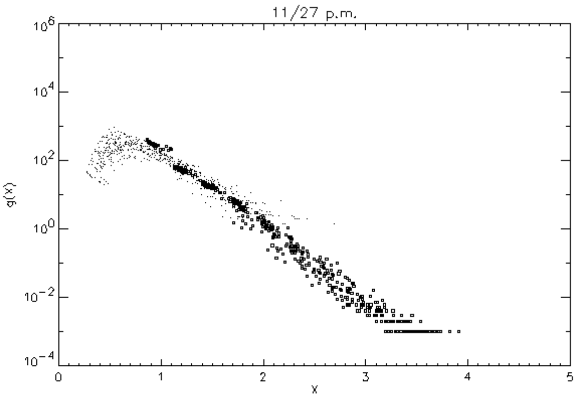
11/27 p.m.
g(x)
10^6
10^4
10^2
10^0
10^{-2}
10^{-4}
0
1
2
3
4
5
x